Deciphering the Energy Use Channels in Soil Organic Matter: Impacts of Long-term Farmyard Manure Addition and Microbial Necromass Revealed by LC-FT-ICR-MS

Konstantin Stumpf[1], Carsten Simon[1*], Anja Miltner[2], Thomas Maskow[3], Oliver J. Lechtenfeld[1*]

[1] Department of Environmental Analytical Chemistry, Research Group BioGeoOmics, Helmholtz Centre for Environmental Research-UFZ, 04318 Leipzig, Germany
[2] Molecular Environmental Biotechnology, Research Group Microbial soil and sediment processes, Helmholtz Centre for Environmental Research-UFZ, 04318 Leipzig, Germany
[3] Microbial Biotechnology, Research Group Ecothermodynamics/Biocalorimetry, Helmholtz Centre for Environmental Research-UFZ, 04318 Leipzig, Germany

*corresponding authors: Oliver Lechtenfeld (Helmholtz Centre for Environmental Research-UFZ, Permoser Straße 15, 04318 Leipzig, Germany, email: oliver.lechtenfeld@ufz.de), Carsten Simon (Helmholtz Centre for Environmental Research-UFZ, Permoser Straße 15, 04318 Leipzig, Germany, email: carsten.simon@ufz.de)

Graphical Abstract

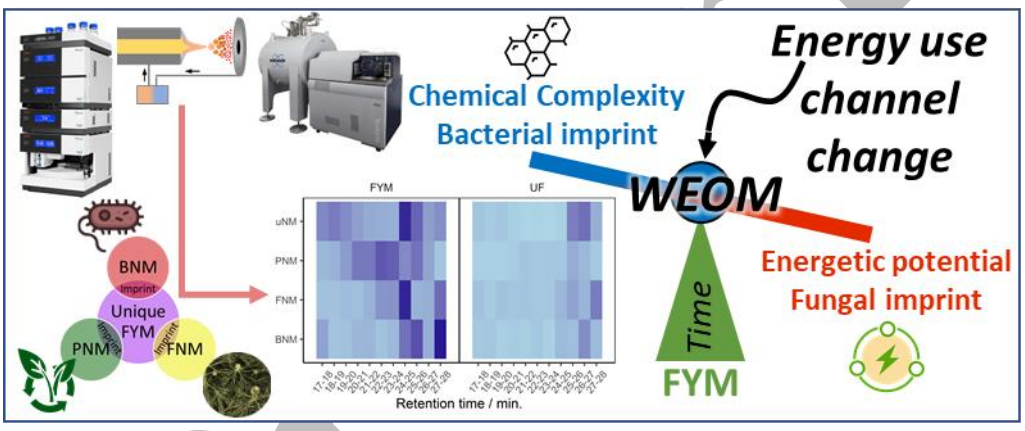

Abstract

Soil organic matter (SOM) plays a central role in the global carbon cycle and contributes to storage of C and energy in soils. Farmyard manure (FYM) addition to arable soils is a measure to increase SOM content, microbial activity and abundance of microbial metabolites (e.g., necromass (NM) markers). However, understanding the mechanistic links between soil dynamics and energy storage is hampered due to the chemical complexity of SOM. Non-targeted molecular-level methods like liquid chromatography coupled to Fourier transform ion cyclotron resonance mass spectrometry (LC-FT-ICR-MS) can be used to explore the complex dynamics of SOM, revealing energetic fingerprints and long-term changes in SOM due to FYM addition. We compared water-extractable organic matter (WEOM) from soils of four long-term FYM addition experiments with representative WEOM signatures from maize, bacterial and fungal NM. Long-term FYM addition increased the complexity of WEOM, most pronounced in polar, unsaturated, oxidised and energy-poor compounds. These changes were linked to a 2-3-fold increase in bacterial, plant and fungal NM signatures. Especially bacterial NM in FYM-amended WEOM indicated a shift in dominant energy use channels. Control soils showed a much lower overlap with all NMs, but indicated a higher dominance of fungal energy-use channels, especially for N-containing compounds. A large fraction of WEOM signals (79% in FYM-amended, 94% in control

soils) was unrelated to any of the three NM signatures, and was also mainly responsible for the shift in nominal oxidation state of carbon (NOSC) between the fertilisation treatments. LC-FT-ICR-MS provided access to ~600 novel microbial NM markers which are readily soluble and compositionally distinct from classical NM markers (ergosterol, aminosugars, etc.). Overall, we highlight novel insights into NM contribution to SOM by LC-FT-ICR-MS, and how it can assist to constrain compositional and energetic impacts of FYM addition on soils.

Keywords

Metabolomics, Ultrahigh Resolution Mass Spectrometry, Turnover, Endmember, Thermodynamics, FT-ICR-MS

Highlights

- Water-extractable organic matter became more soluble, oxidized and chemically complex after FYM treatment
- Farmyard manure addition led to an increased imprint of necromass markers in soil WEOM
- Bacterial imprints increased over fungal ones, suggesting changes in C, N and energy use channels
- Lower energetic potential of soil WEOM was explained by compounds unrelated to necromasses, indicating potential priming
- LC-FT-ICR-MS provided access to 600 novel, readily soluble bacterial and fungal necromass markers

1. Introduction

There is a growing interest in the origins and energetic properties of stable soil organic carbon (SOC). This interest comes from the crucial role that SOC plays in soil ecology, providing important ecosystem services such as soil fertility, water quality, resistance to erosion, and climate mitigation (Kögel-Knabner and Rumpel, 2018). Understanding the dynamics of stable SOC has therefore become paramount in addressing global change (Schmidt et al., 2011) since global soils contain 3000 Pg and therefore more organic C than present in the atmosphere as CO_2 or as organic C in biomass (Tarnocai et al., 2009; Schmidt et al., 2011). Our understanding of SOC dynamics is represented by models that presume distinct C pools cycling fast or slow, but only partly reflect the complex mixture referred to as soil organic matter (SOM) (Schmidt et al., 2011; Lehmann and Kleber, 2015). Recent studies soggest that stable SOM formation is tied to the metabolic activities of microorganisms, giving rise to a diverse array of compounds, including microbial necromass (NM) and plant-derived, microbially processed compounds which may hold clues of active C and energy use channels (Guggenberger et al., 1999; Kögel-Knabner, 2002; Miltner et al., 2012). Models assign a large fraction of microbial NM to stable SOM now (Malik et al., 2016; Craig et al., 2018; Liang et al., 2019). This is supported by studies using nuclear magnetic resonance spectroscopy (Simpson et al., 2007), stoichiometric properties (Del Giorgio and Cole, 1998), amino sugars (Fan and Liang, 2015), turnover of microbial proteins and cell structures (Schweigert et al., 2015), and contribution of microbial products to stable SOM (Kästner and Miltner, 2018; T. Ma et al., 2018). Next to microbial (exo)metabolites, also microbial NM (e.g., colloidal proteins or ribosomes) contributes to the water-extractable fraction of SOM (WEOM). This fraction is deemed the most active and biologically-accessible component of SOM (Ma et al., 2020). WEOM therefore is a mirror of microbial activity, and linked to primary and secondary metabolites such as carbohydrates, amino acids, nucleosides, sterols, arenes, amines, and many other, yet unidentified molecules (Schmidt et al., 2011). Due to its intermediate position between biochemically recognizable compound classes and their mineralization products (CO_2, H_2O, etc.), it can potentially serve to improve our understanding

of the imprints of sources and processes that affect SOM composition and stability in general (Reemtsma et al., 2006).

Global agriculture produces nearly seven billion tons of farmyard manure (FYM) annually (Thangarajan et al., 2013). The application of FYM increases SOC and nutrient contents and has been reported to also increase microbial activity, microbial metabolite abundances, and amounts of extractable SOC . The increase in C storage has been assigned to more NM formation due to better access to labile substrates and nutrients (Chang et al., 2007; Maillard and Angers, 2014). The mechanism by which the increased microbial activity affects the composition of WEOM and SOM stabilization in general remains unclear due to the largely unknown identity of most molecules in soils and NM. Metabolomic techniques have been applied to resolve these molecular imprints and are deemed promising to provide mechanistic understanding of molecular-level foundations of biogeochemical processes like C and nutrient cycling, or novel measures to evaluate soil health (Brown et al., 2024). These metabolomics studies could also provide information of changes to the energetic potential of WEOM (via nominal state of oxidation of C, NOSC which is empirical correlated with Gibbs free energy), and by comparison with NM markers, could reveal causal links between WEOM properties and active C and energy use channels (LaRowe and Van Cappellen, 2011; Gunina and Kuzyakov, 2022). Chromatographic techniques coupled to mass spectrometry (GC-MS, LC-MS), for example, allow to identify molecules via libraries of known compounds, but a majority of the information is left unassigned (Swenson et al., 2015; Brailsford et al., 2019; Brown et al., 2021).

Ultrahigh resolution mass spectrometry such as Fourier transform ion cyclotron resonance mass spectrometry (FT-ICR-MS) allows for the assignment of molecular formulas independent of libraries due to its unmatched mass precision and resolving power, and can be coupled to LC systems (Bahureksa et al., 2021; Lohse et al., 2021). Due to its analytical performance, it could complement existing metabolomic techniques that rely on library identification and are targeted at known compound classes (e.g., amino sugars, peptides, or biomarkers in general). FT-ICR-MS techniques have been employed successfully to study SOM extracts by direct injection (Tfaily et al., 2015; Guigue et al., 2016; Roth et al., 2019; Lohse et al., 2020; Zhang et al., 2021). The two main drawbacks of this approach are the often necessary preconcentration step performed by solid-phase extraction (SPE), which typically suffers from uncomplete recovery (losses of highly polar compounds (Raeke et al., 2016)), and the missing confidence in the structural identity of matching NM and SOM markers, as they are only identified via molecular formula (i.e., exact mass). The coupling of FT-ICR-MS with LC is therefore promising as it avoids SPE, i.e., allows on-line separation of salts from organic molecules, and increases sensitivity and isomeric resolution (Jennings et al., 2022; Lechtenfeld et al., 2024). Using LC-FT-ICR-MS for WEOM analysis will be likely result in identifying a broader spectrum of molecules resulting in a higher confidence of NM assignment (i.e., distinction from other WEOM molecules) due of the added polarity information. While WEOM is typically measured in negative ESI mode due to abundant carboxylic acid groups, N-rich metabolites are usually missed but can be selectively detected by also employing positive ESI mode (Ohno et al., 2014). The method therefore is appropriate to complement existing targeted approaches, and may provide novel insights to decipher the links between microbes and WEOM compositional changes upon long-term FYM addition.

To 1) identify NM markers in WEOM and to 2) compare NM marker contribution between FYM receiving soils and controls, we employed a state-of-the-art LC-FT-ICR-MS method and compared WEOM from soils and NM samples. We analysed WEOM from FYM-receiving soils (FYM) and control soils being unfertilized (UF = *nil* fertilization), as well as necromass (NM) extracts derived from plant litter (PNM, *Zea mays*), bacteria (BNM, *Bacillus subtilis*), and fungi (FNM, *Aspergillus niger*). We chose to use both electrospray polarity modes to detect acidic as well as basic compounds (Hertkorn et al., 2008; Han et al., 2021). Our main hypothesis was that FYM-receiving soils would show markedly

different molecular properties, regarding molecular composition and NOSC of the extractable compounds. Further we hypothesised that these differences in energy and structure would be explained through higher contributions of yet unknown plant, bacterial and fungal NM markers, which would provide clues on the impacts of FYM addition, and the role of soil microbes as important drivers of FYM and SOM turnover.

We show the distinct impacts of long-term FYM addition on WEOM regarding its NOSC, polarity, saturation, nitrogen and oxygen content, molecular size and overall complexity. We expected that increased contributions of NM would relate to these observed differences in WEOM character. The NM signatures are then used to reveal the relative importance of different WEOM sources, according to their share in ion abundance, which we refer to as "imprint". Our findings offer a novel molecular perspective on the roles of microbial, fungal and plant-derived compounds and their contribution to long-term SOM formation and changes.

2. Materials and methods

2.1. Substrates and soil samples

Soil samples were taken from four long-term field experiments: Dikopshof (University of Bonn, Germany, established 1904), Reckenholz (ZOFE, Agroscope, Zurich, Switzerland, established 1949), Thyrow (Humboldt University, Berlin, Germany, established 1937) and QualiAgro (INRAe, Orgeval, France, established 1998) (Table S1). From all four field trials samples were taken from plots that continuously receiving farmyard manure ("FYM") and control plots ("UF", plots receiving *nil* fertilizer but else treated similarly). Samples were taken in 2020 from 2-20 cm depth. The measured necromass (NM) samples were bacterial necromass (*Bacillus subtilis*, BNM), fungal necromass (*Aspergillus niger*, FNM) and plant necromass (*Zea mays*, PNM). FNM was purchased (Isolife, Wageningen, Netherlands). PNM was produced by growing the variety "Yukon Chief" in hydroponic pots with a modified Hoagland nutrient solution at a temperature of 20°C in a greenhouse at Max Planck institute for Biogeochemistry in Jena Germany. The plants were harvested after cob formation and aboveground plant parts were separated, cut, freeze dried and milled. BNM was produced by ultrasonically disintegrating *Bacillus subtilis* DSM 10 cells. Briefly, *B. subtilis* was grown aerobically at 30.0±0.003 °C in a 1.5-liter bioreactor (RC1e (Mettler Toledo, Greifensee, Switzerland) in fed-batch mode on a mineral medium with glucose as the sole C and energy source. The usage of the bioreactor allowed growth to a high cell density. When the culture volume reached 1.5 L, the cells were harvested by centrifugation at 12,000 g and 4°C for 20 min and washed with phosphate-buffered saline. The resulting biomass was freeze-dried.

2.2. Extraction of necromass and soil samples

All aqueous extracts were obtained by suspending 1 g of dry sample in 10 ml of ultra-pure water (MQW; Merck Milli-Q, Darmstadt, Germany). Suspensions were shaken for 24h followed by centrifugation (4500 g for 20 min, Beckman Coulter, United States) and filtration (0.2 µm, regenerated cellulose, LABSOLUTE). The filtrate was used for further analysis. In the following, WEOM refers to the aqueous extracts of the field trials, while necromass extracts refers to the aqueous extract of the microbial necromass samples. Water-extractable organic carbon (WEOC) was determined with a Dimatoc 2100 (Dimatec, Essen, Germany) system as non-purgeable organic carbon by near–IR absorption after high temperature catalytic oxidation according to EN 1484. Five ml of each sample were acidified with 2 µl of 37% HCl (p.A., CHEMSOLUTE) to remove inorganic C before NPOC analysis. The concentrations and extraction yield of samples are provided in the supplement (Table S1).

2.3. Reversed Phase Liquid Chromatography (RP-LC)

An UHPLC system (UltiMate 3000RS, Thermo Fischer Scientific, Waltham, MA) equipped with a binary pump (HPG-3200RS), a column oven (TCC-3000RS), an auto sampler (WPS-3000TRS), and a

diode array detector (DAD-3000RS) was used. A reversed phase polar end-capped C_{18} column (ACQUITY HSS T3, 1.8 µm, 100 Å, 150 × 3 mm, Waters, Milford, MA) equipped with a guard column (ACQUITY UPLC HSS T3 VanGuard, 100 Å, 1.8 µm, 2.1 mm × 5 mm) was used for chromatographic separation. Ultra-pure water and LC-MS-grade methanol (MeOH; Biosolve, Valkenswaard, Netherlands) were used as mobile phases A and B, respectively. 0.1% formic acid (FA) was added to both eluents. A second LC pump (LPG-3400SD) was used to add a post column flow (0.2 mL/min). A gradient was applied as to reverse the gradient of the first pump at the column outlet using the same solvents (A: MeOH, B: MQW). The combined flow (50% MQW, 50% MeOH) was separated between the mass spectrometer (0.1 mL/min) and DAD (0.3 mL/min, 210-280 nm) using an adjustable flow splitter (ERC, Germany) (information about gradient and counter gradient found in Han et al., 2021). Filtered WEOM-extracts were diluted to 10 mg-OC/L, and 100 µl of the diluted extracts was injected into the UHPLC system.

2.4. FT-ICR-MS

An FT-ICR-MS equipped with a dynamically harmonized analyser cell (solariX XR, Bruker Daltonics Inc., Billerica, MA, USA) and a 12 T refrigerated actively shielded superconducting magnet (Bruker Biospin, Wissembourg, France) was used. The electrospray ionization source (Apollo II, Bruker Daltonics Inc., Billerica, MA, USA) was operated in negative (neg) or positive (pos) mode (capillary voltage: 4.3 kV (neg) or -4.3 kV (pos), nebulizer gas pressure: 1.0 bar, dry gas temperature: 250 °C, dry gas flow rate: 8.0 L/min), and each sample was measured in both modes separately. Mass spectra for LC-MS measurements were acquired in broadband excitation mode and detected in the range m/z 147.41 - 1000 with a transient size of 4M (~1.86s FID) and full profile, magnitude mode. Each sample and polarity were measured as duplicate.

2.5. FT-ICR-MS data processing

LC-MS data was split into eleven one-min wide retention time (RT) segments between 17 and 28 min and all scans in each segment were averaged. This retention time span was selected because it showed the largest overlap between positive and negative mode, across all samples. Peak picking signal to noise (S/N) threshold was 4 in each segment. Each resulting mass spectrum was internally recalibrated with a list of ubiquitous, known signals between 150−1000 m/z. Mass spectral calibration of segments was done with DataAnalysis 5.0 (Bruker Daltonics Inc., Billerica, MA, USA). Molecular formulas (MFs) were assigned to mass peaks in the m/z range 150−1000 using the n in-house software Lambda-Miner (Wurz et al., 2024), allowing for a maximum mass error of ±0.5 ppm and the following elemental ranges: C_{1-60}, $^{13}C_{0-1}$, H_{1-122}, O_{0-40}, N_{0-2}, S_{0-1}, $^{34}S_{0-1}$. Additional filters were applied to the calculated MFs: 0.3 < H/C < 2.5, 0 < O/ C < 1, 0 < N/C < 1.5, 0 < DBE < 25 (double bond equivalent, DBE = 1 + 1/2 [2C − H+N]), −10 < DBE-O < 10 and element probability rules (Kind and Fiehn, 2007; Herzsprung et al., 2014; Koch et al., 2014). MFs assigned to peaks in MQW injections were removed from each segment. Duplicate sample injections were averaged and only MFs kept that occurred in both replicates. This procedure was done for both ionisation modes separately, and the data from both modes was then combined (*union*) for further analysis. To obtain the MFs that occur uniquely in UF extracts, data from all field-trial sites was pooled, and a first Venn analysis was conducted to define sets of MFs for each RT segment occurring only in UF or FYM samples (*unique*) or both (*shared*). Only the MFs unique to UF or FYM in each segment was considered informative to reveal differences between treatments (Figure 1). A second Venn analysis was then conducted to reveal the overlap of unique FYM and UF signatures with those of NM extracts (BNM, FNM and PNM; Figure 1). Only the shared MFs were considered informative for the further analysis. Markers that were found to overlap with soil WEOM and were also found in more than two (i.e., two or three) NM extracts were grouped as an own category (uNM). This category is used to indicate generic NM contribution.

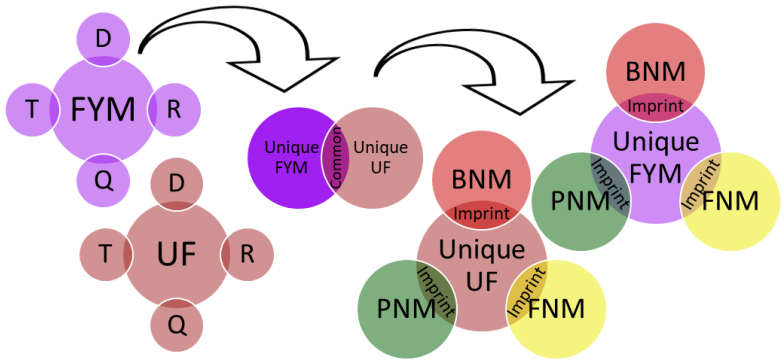

Figure 1: Overview of the applied data sub-setting procedure through a two-step Venn analysis. First step (left): Union of all measured soil sampling sites (Dikopshof (D), Thyrow (T), Reckenholz (R), QualiAgro (Q)) according to fertilisation mode (fertilised (FYM), control (UF)). Second step (middle): Difference of acquired FYM and UF sets to obtain signals unique to FYM and UF. Third step (right): Intersection of unique signals of UF and FYM with necromasses (NMs) (bacterial (BNM), plant (PNM), fungal (FNM)) to obtain imprints specific to each NM within FYM and UF soil samples.

3. Results

3.1. Differences in polarity, complexity and composition of WEOM

Farmyard manure-receiving (FYM) and control (UF) soils showed distinct WEOM molecular and polarity patterns according to LC-FT-ICR-MS analysis (individual chromatograms are shown in the supplementary information Figure S1 – S11). The summed intensity of all MFs per RT segment showed a similar increase in intensity from smaller to higher retention time and peaked at 24 – 27 minutes, but the overall intensity was always 1.5 to 2-fold higher for FYM than for UF (Figure 2a) despite the same amount of injected OC. The higher intensity of FYM extracts corresponded to the larger number of assigned unique MFs across all RT segments as compared to UF extracts (29242 vs. 5580; 57 vs. 11% of all MFs in each treatments) and especially increased in the time range 17 – 24 min (Figure 2b). 16977 MFs were shared between both treatments (Figure 2a).

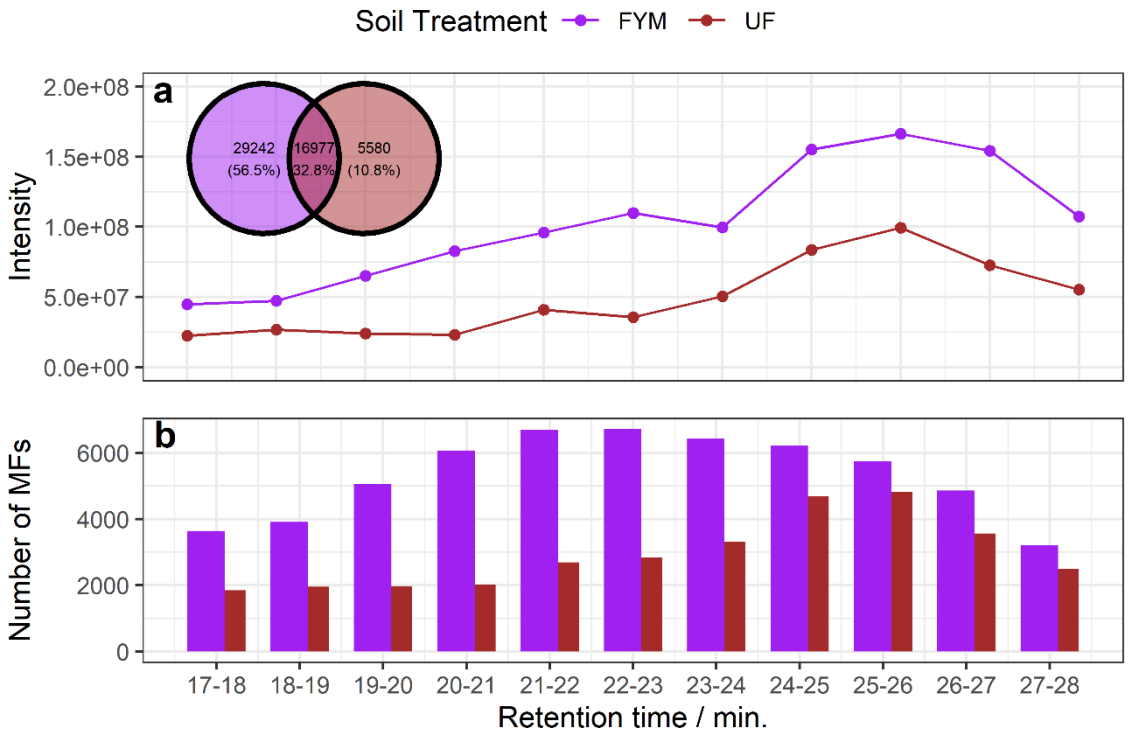

Figure 2. Comparison between fertilised (FYM, purple) and unfertilised (UF, brown) WEOM molecular composition as observed from LC-FT-ICR-MS, showing merged data of both ESI- and ESI+ modes. (a) The summed intensity of all assigned molecular formulas (MFs) of UF and FYM per retention time segment. Inset Venn diagram shows the numbers of unique and shared MF between UF and FYM WEOM. (b) The number of unique MFs per segment for UF and FYM. The shared MFs are not shown.

To further explore the molecular differences between MFs unique to FYM and UF, we compared the intensity weighted-averages of atomic ratios (O/C, H/C, N/C), the nominal oxidation state of carbon (NOSC), the double bond equivalents (DBE) and molecular weight for each segment across the observed polarity range (Figure 3 and Figure S12). In general, reversed-phase LC separation led to clear continua in all of the above molecular descriptors for each sample. Upon comparison of the treatments, we found a pronounced shift to higher NOSC, higher O/C and lower H/C across virtually all RT segments in WEOM from the FYM treatment (Figure 3). Other molecular descriptors indicated small, but specific differences. For example, N/C was consistently higher in FYM only in the first three RT segments (highly polar material), along with a tendency to lower average molecular mass (Figure S12a, c), while DBE was consistently higher in FYM samples only in the mid-polarity range (Figure S12b). All in all, compositional differences between WEOM samples were consistent across the whole polarity range, but not statistically significant (Figure S13). The clear shift in virtually all polarity segments indicates that WEOM from FYM soils is more oxidized and less saturated, resulting in higher NOSC values. The molecular variability was highest in FYM extracts and earlier-eluting material (Figure 3). Differences between treatments were also most obvious in the early-eluting RT segments (more polar WEOM). In contrast, later eluting (less polar, more reduced) compounds indicated less differences between treatments.

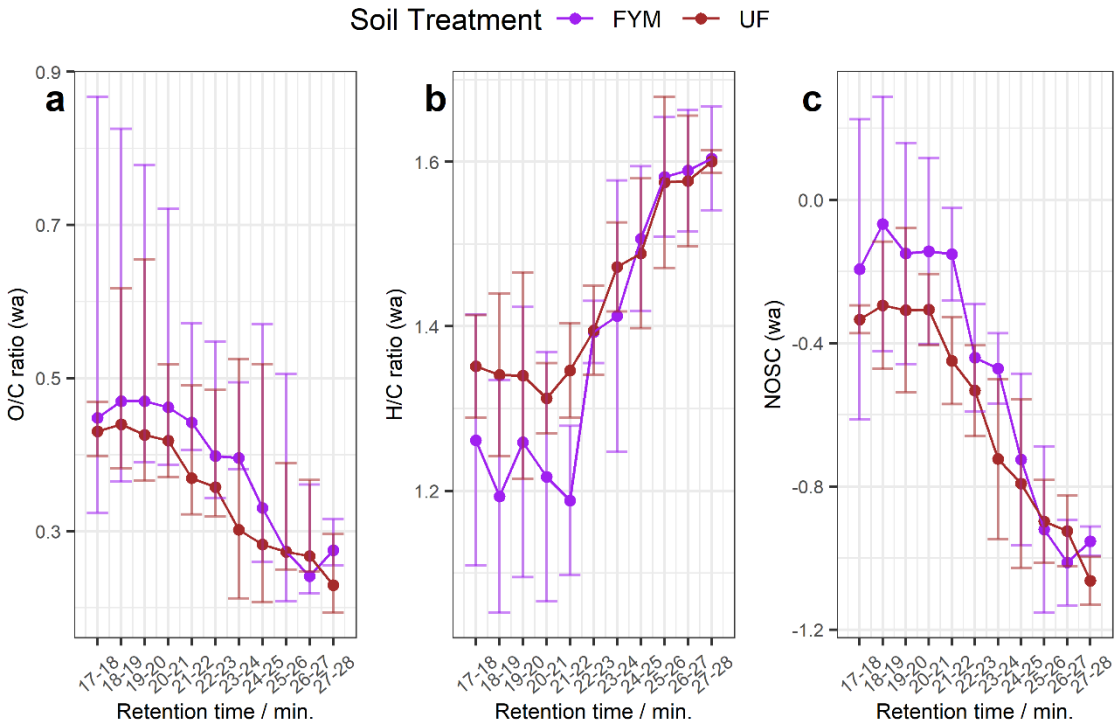

Figure 3. Aggregated (intensity-weighted average) molecular descriptors of WEOM for individual LC-FT-ICR MS segments (17-28 min, n = 11). (a) oxygen to carbon (O/C) ratio, (b) hydrogen to carbon (H/C) ratio, (c) nominal oxidation state of carbon (NOSC). Data is shown for molecular formulas (MFs) unique to unfertilized (UF, brown) and fertilized (FYM, purple) WEOM. The means (dots) and standard deviation (error bars) were determined from the different field trials (n = 4).

3.2. Molecular composition of BNM, FNM and PNM

We also characterised bacterial, fungal, and plant necromass extracts regarding unique MFs (BNM, FNM and PNM) and shared MFs (uNM) according to H/C ratio, O/C ratio, N/C ratio, DBE, molecular mass and NOSC for each RT segment (Figure S14). FNM and BNM appeared more similar compared to PNM and differed most in polar unsaturated compounds (high DBE values in early RT segments Figure S14e) and polar higher-mass compounds (Figure S14f). BNM and FNM showed equal patterns in N/C-ratio, NOSC and O/C-ratio (Figure S14a-d). In contrast, PNM showed compounds with smaller N/C-ratio compared to FNM and BNM, especially in the later RT segments (Figure S14c), more reduced polar and more oxidised nonpolar MFs than BNM and FNM (Figure S14d) and more polar oxygen-containing compounds than BNM and FNM (Figure S14a) that were also more saturated (Figure S15b). Those differences were also apparent in the PCA (Figure S15) and all NMs were mainly divided by NOSC, O/C ratio, N/C ratio and DBE. This clear division between NM samples according to measured molecular descriptors is visible within the PCA as dimension 1 separates uNM from all other specific NM types and dimension 2 separates PNM, BNM and FNM from each other. Overall, based on detailed LC-FT-ICR-MS analysis, FNM and BNM were more similar in composition with PNM, differing mainly in saturation, but showed very similar N/C ratios (high) and NOSC (low). PNM was distinctly more oxidised and contained more saturated compounds as compared to FNM and BNM. Shared NM markers (here called "uNM", found in at least two NM extracts) showed especially high N/C ratios in earlier RT segments and an increase in mass towards later RT segments; this group of markers was also especially low in DBE across the whole polarity gradient (Figure S14).

3.3. Imprints of necromass in SOM extracts related to FYM addition

In the next step, we characterised those NM markers also detected by exact mass (molecular formula) and RT segment in WEOM ("overlap" in MFs). To visualise the impact of NM markers as defined by our two-step Venn analysis (Fig. 1), we displayed their intensity share (in %) in WEOM according to RT segment, and for UF and FYM soils separately (Figure 4a). We found a larger overlap of NM markers with FYM WEOM throughout the entire polarity gradient and for all NM types. Shared NM markers between NM types (uNM) showed high overlap in early and late RT segments, and in UF soil WEOM only in later RT segments. Especially PNM and BNM showed a higher overlap (intensity-wise) with FYM WEOM, while FNM showed higher overlap with UF extracts in later RT segments. PNM showed overlap with all soil WEOM, but in FYM extracts this occurred throughout the whole polarity gradient, accounting for 5%-10% of the total intensity in 10 out of 11 RT segments (Figure 4 a). In contrast, a high PNM imprint (5-10%) was confined to only two later time windows in UF extracts. The BNM imprint accounted for 5-15% in 4 out of 11 RT segments in FYM extracts, while it was below 5% within the entire retention time span for UF extracts. Lastly, we found that the FNM imprint was between 4% and 8% for 4 out of 11 RT segments in UF extracts. All in all, our data show a much larger and more variable imprint of necromass signatures in FYM-receiving soils. Importantly, a major fraction of intensity remained unexplained, i.e., showed no overlap with any of the NM markers, even after consideration of shared (uNM) markers (75% - 90% for FYM and 90-95% for UF) (Figure 4b).

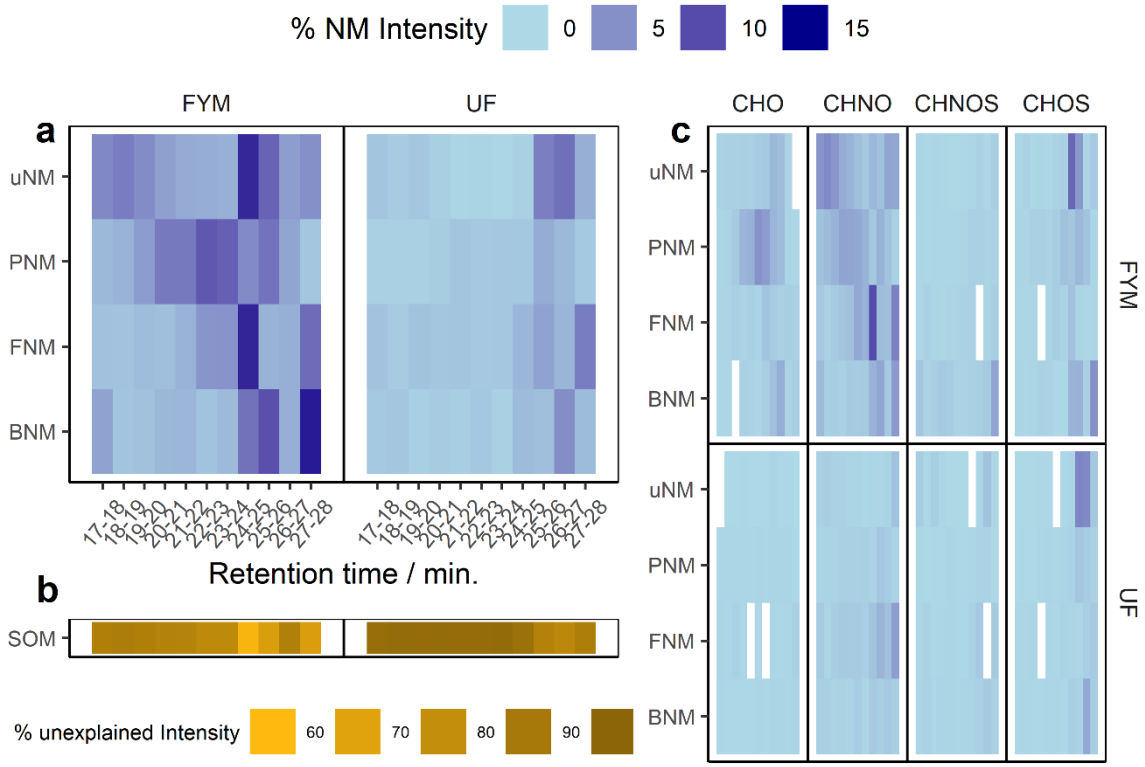

Figure 4: Necromass (NM) marker in WEOM from unfertilized (UF) and fertilized (FYM) field trials. (a) Fraction of intensity of molecular formulas (MFs) unique to FYM (left panel) and UF (right panel) represented by NM-related MF in each LC-FT-ICR MS-derived segment. (b) Intensity fraction of MFs unique to FYM (left panel) and UF (right panel) that is not derived from NM-related MFs (collectively referred to as "SOM"). (c) Fraction of NM-related MFs intensity split according to formula classes (CHO, CHNO, CHNOS, CHOS) and FYM (top panel) and UF (bottom panel). Y-axes in (b) and (c) same as in (a). No available data (i.e., no MFs found in respective segment) is shown in white, other percentual input is shown in blue or golden colour gradient (from light colour shade = 0% NM imprint to dark colour = highest percentual imprint).

In terms of formula classes (using heteroatom information, i.e., containing N or S atoms), the CHNO formula class showed the highest contribution of NM-derived MFs in both treatments, but some shared (uNM) and S-containing markers were also abundant (Fig. 4c). Fungal NM markers had the highest impact on the measured intensity of MFs classified as CHNO (20% for FYM and 24% for UF). In WEOM of UF soils, we found no substantial contribution of any NM and formula class despite FNM/ CHNO, i.e, all remaining contributions accounted for less than 4% of intensity. Therefore, the change compared to FYM soil WEOM, in which BNM and PNM also contribute to a high degree to CHNO formula classes (16% BNM and 14% PNM) indicated a distinct difference in composition between the treatments. The contribution of NM markers to specific formula classes indicated a shift towards BNM and PNM contributions in FYM soil WEOM extracts compared to those of UF soils, especially for the CHNO formula class. Other formula classes showed higher PNM contribution in FYM-amended soil WEOM. A fraction of late-eluting CHOS MFs shared between NM types (uNM) was elevated in both treatments; in FYM-amended soil WEOM extracts, also unique BNM contributions were more apparent.

Averaged molecular descriptors of NM markers in WEOM samples were visualized to estimate the impact of NM to the molecular-level differences between treatments, specifically of NOSC (Fig. 5a). Four observations were made: 1) The H/C ratio was consistently higher for all marker categories (unique NM markers: BNM, FNM, PNM, shared NM markers: uNM, unexplained MFs: SOM) in UF WEOM as compared to FYM-amended WEOM (Figure 5a); 2) FYM WEOM had consistently higher NOSC values as compared to UF treatments and differed most for PNM and uNM markers (Figure 5a); 3) Considering these changes in NOSC and the intensity share of each category, the influence on NOSC across the entire polarity spectrum was mainly explained by compounds in WEOM that showed no

overlap with NM signatures (Figure 5b), and 4) The observed shift in NOSC was mainly linked to the contribution of highly polar compounds in earlier segments (17-21 min). BNM and FNM showed a slight influence on NOSC in FYM samples (Figure 5b) and the overall shift in NOSC compared to UF WEOM, but this was confined to the early RT segments and comparably small (Figure 5 c).

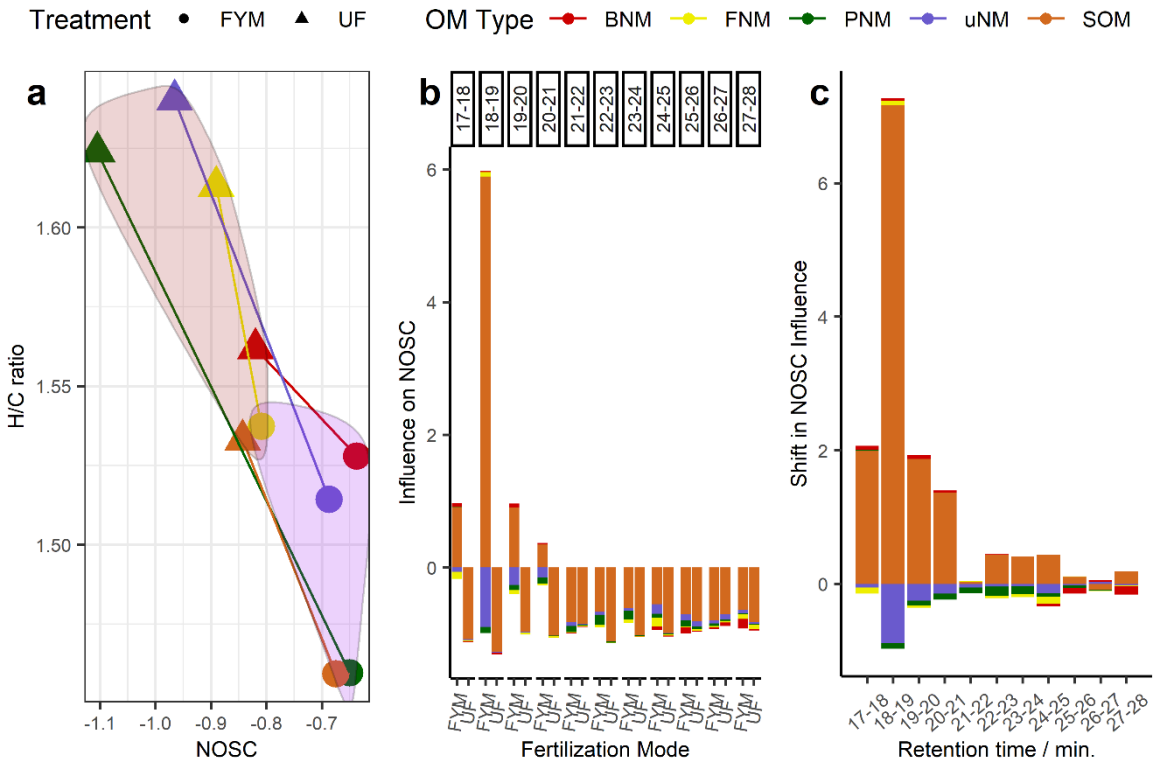

Figure 5: NOSC shifts in fertilized (FYM) and unfertilized (UF) soils linked to the influence of NM marker. (a) Intensity-weighted averages of molecular hydrogen to carbon (H/C) ratio and nominal oxidation state of carbon (NOSC) of NM imprints and remaining SOM imprints in soil WEOM extracts for unique plant (PNM, green), fungal (FNM, yellow) and bacterial markers (BNM, red), shared markers (uNM, purple), and remaining markers (i.e., not associated with NM, referred to as "SOM", orange). FYM-receiving WEOM is shown by circles and UF WEOM by triangles. Highlighted envelops represent the range of the above five categories in FYM (purple) and UF (brown) WEOM. (b): Influence of NM and SOM imprints on average NOSC across LC-segments. Calculated as ratio of NOSC of NM or SOM imprint to general weighted mean of NOSC of FYM or UF per segment, weighted by intensity share (Figure 4). (c) Change in influence of NM and SOM imprints between FYM and UF WEOM on NOSC calculated as difference per imprint group from (b).

4. Discussion

4.1. Effects of long-term FYM addition on WEOM molecular properties

It is known that FYM addition increases SOC stocks, the amount of extractable SOC, microbial activity as well as microbial biomass (Q. Ma et al., 2018; Liu et al., 2020). The increase in SOC results in greater amounts of microbial NM that contribute to SOC. Bacterial NM accounts for approximately half of SOC within croplands (Wang et al., 2021). Given the more reduced state of bacterial NM, one would expect that long-term FYM addition also leads to a more reduced (i.e., energy-rich) SOM, and hence WEOM (Tang et al., 2023). Although FYM-receiving soils were characterized by a 63% increase in WEOC as compared to the UF soils, higher richness in terms of formulas detected (especially in the mid-polar region, Fig. 2) and 10% larger overlap with NM markers (Figure 4), WEOM was more oxidized due to FYM addition (Fig. 3c). This indicates that the FYM treatment increased the number of water-soluble compounds, which generally tend to be more oxidized, hence explaining higher content and NOSC of WEOM and relative WEOM to SOC ratio. This is reflected on a structural level as FYM treatment led

to a more polar, higher oxidized pool of WEOM compounds (higher O/C, lower H/C, higher NOSC; higher N/C and lower mass of the most polar compounds, Fig. 3, Fig. S12). The differences between treatments became undetectable for the least polar and most reduced compounds (Fig. 3c). Similar shifts to more oxidized extractable OM upon long-term FYM addition were based on FT-IR spectroscopy, indicating increased carboxyl-C contents (Kaiser and Ellerbrock, 2005; Ellerbrock et al.). Higher amounts of WEOM and hydrophilic aliphatic compounds (e.g. long-chain carboxylic acids) were also found after green manuring (Sharma et al., 2017). On the contrary, also presumably less mobile fractions were found to be more responsive to long-term FYM addition, e.g. an enrichment of nonpolar alkyl compounds (likely fatty acids) and peptides at the expense of aromatics (Mao et al., 2008) or an increase in peptide- and RNA/DNA-related small metabolites in organic SOM extracts (Tang et al., 2023). Our results from direct analysis of WEOM with LC-FT-ICR MS indicate that the most mobile fraction of SOM (i.e., WEOM) shows a consistent response to long-term manuring.

The observed difference between FYM-treated soils and unfertilized controls can be explained by the higher microbial activity leading to an increased oxidation of SOM. Like shown related to temperature higher microbial activity is linked to higher DOC levels in soils (Kalbitz et al., 2000). Microorganisms utilize readily available compounds with neutral to positive NOSC values (carboxylic acids, sugars and some amino acids) to fuel their metabolism while reduced compounds and NM, as a result of anabolism followed by cell death, may accumulate to form less soluble SOM that requires oxidation prior to reuse (Gunina and Kuzyakov, 2022). Alternatively, manure itself is enriched with readily bioavailable compounds which could explain higher NOSC values of WEOM in FYM-receiving soils. A more oxidized WEOM may therefore indeed relate to an indirect effect of increased microbial oxidative consumption of SOM initiated by long-term FYM addition.

Altogether we found that FYM addition favoured a WEOM composition that appears readily available to bacteria or fungi. Since WEOM can be seen as a link between SOM pools, our findings point to an increased potential for bacterial and fungal sequestration of C, in line with studies showing increased SOC and nutrient storage, soil enzyme activity and microbial biomass in FYM-receiving soils (Hu et al., 2024). On the other hand, our findings also indicate a loss of energy-poor SOM at the expense of an increased microbial activity leading to the formation of SOM dominated by microbial NM. This would suggest parallel priming (mineralisation of beforehand stable C) of existing SOM at the expense of a build-up in necromass.

We therefore discuss if the molecular changes to WEOM are explained by an increased imprint of a) bacterial or fungal NM markers (i.e., NM recycling following specific energy-use channels), b) litter markers (increased leaching from plant NM) or c) unknown WEOM markers (potential SOM decomposition products, possibly indicating processes such as priming).

4.2. FYM addition increases the share of NM markers in WEOM

Our data suggest an overall higher contribution of necromass to FYM-receiving as compared to control soil WEOM (Fig. 4). Compared to control soils, the combined overlap of these markers was increased by 3.0%, 2.5% and 1.6% for plant, bacterial and fungal NM maker, respectively, suggesting a stronger increase of bacterial vs. fungal activity and an increased availability of soluble plant metabolites. Additionally, shared markers between NM types (uNM) were increased by 3.5%, suggesting a general increase in metabolites due to higher biotic activity. Together, NM markers therefore explained 10.7% more intensity in FYM-receiving soil WEOM than in controls (i.e., 17.1% vs. 6.4%). The range of overlapping markers extended to much more polar and oxidized compounds (earlier RT segments, Fig. 3c) than in control soil WEOM, where it was confined to later eluting, reduced compounds (Fig. 4a), thus explaining increased NOSC levels (Fig. 3c). Interestingly, in control soils, the nonpolar, reduced S-containing compounds ("CHOS") belonged to BNM and uNM, while nonpolar, reduced N-containing

compounds ("CHNO") were mainly linked to FNM, and no distinct overlap with CHO compounds (containing neither S nor N) was found (Fig. 4c). In contrast, FYM-receiving soil WEOM showed a wider NM imprint of CHNO compounds with all NM types (uNM and PNM: polar, oxidized compounds; FNM and to a lesser extent BNM: nonpolar, reduced compounds); nonpolar and reduced CHOS compounds were similarly linked to uNM and BNM fingerprints, and relatively polar CHO compounds were linked mainly to the PNM fingerprint (Fig. 4c). The higher number of CHNO compounds likely reflects a greater microbial activity in FYM-treated soils generally, since microbial NM consists of residues or by-products of intact or ruptured cells or hyphae, as well as monomers or polymers found within the cytoplasm, biofilm, or hyphal mucilage, such as polysaccharides (peptidoglycan or chitin), proteins (including enzymes), and DNA (Buckeridge et al., 2022). A relatively similar overlap of S-containing compounds in both treatments suggests similar S cycling independent of the FYM treatment, and was mainly mediated by nonpolar, reduced forms of S likely related to sulfolipids or long-chain sulfonic acids. An increased fraction of CHO metabolites from plants (PNM) suggests stronger production of leachable compounds from plant litter in FYM-receiving soils. Compared with the NM markers assigned by LC-FT-ICR-MS, original farmyard manure mass spectra (measured by LDI-FT-ICR-MS, (Simon et al., 2024)) potentially contained 56% PNM markers and only 15% BNM markers, supporting the higher overlap with plant necromass. Yet, only an average 6% of NM markers (4% BNM, 6% FNM, 7% PNM and 9% uNM) found in soil WEOM were also found in the original manure mass spectra measured by LDI-FT-ICR-MS, suggesting that leachable NM markers in soils originate from a different source than farmyard manure itself.

Our findings provide evidence of a stronger impact of NM on WEOM in FYM-receiving soils, and suggest that especially oxidized N-containing compounds and plant-related oxidized CHO compounds are differently cycled due to FYM addition, leading to their transfer into the water-extractable, and likely bioavailable, SOM pool. The increased overlap with BNM markers suggests a shift towards an energy-use and N cycling channel dominated by bacteria over one dominated by fungi in non-fertilized soils. N stands out as one of the primary nutrients restricting microbial growth, and it is known that manure application increases fungal and bacterial diversity and enzymatic activity (Ma et al., 2020). It was shown before that bacteria operate predominantly in narrow C:N environments with a labile pool of detritus (here, FYM) while fungi dominate environments with less nutrients available and perform N-mining on more resistant detritus forms (here, SOM in control soils) (Moore et al., 2002). The observed shift from a fungal to a bacterial WEOM imprint could therefore be linked to a shift from fungal N-mining in soils with little nutrient availability to bacterial recycling of easily available N from FYM (Allison et al., 2007; Rousk and Bååth, 2007). Previous studies have demonstrated that fungi tend to decompose recalcitrant SOC, such as lignin and cellulose, and bacteria then utilise the fungal-derived products (Boer et al., 2005). The lack of easily-accessible plant NM-derived compounds in control soil WEOM could be a reflection of the dominant role of fungal NM for N supply in nutrient-deprived control soils (Op De Beeck et al., 2018).

4.3. An extended view of necromass markers in soil WEOM

Amino sugars, amino acids or other N-containing molecules are often used as markers of bacterial and fungal NM (Withers et al., 2020). Among other compounds, muramic acid is an accepted indicator of bacteria, while fungal contribution to SOM pools may be estimated via glucosamine (after correction) or ergosterol (Glaser et al., 2004; Joergensen, 2018; Adamczyk et al., 2024; Salas et al., 2024). Using known fractions of these markers in common microbial cells, one can derive estimates of microbial C/ SOM (Joergensen, 2018; Salas et al., 2024). However, amino sugars only account for about ~5% of N-containing compounds in SOM (Wu et al., 2023). Microbial residues were shown to contribute 15-80% to the stable SOM pool (Liang et al., 2019; Hall et al., 2020; Angst et al., 2021). Our data suggest only 2-25% (average 7.9%) and 0-15% (4.8%) of unique microbial NM (= BNM + FNM) in FYM-receiving

and control soil WEOM, respectively. While this estimate based on molecular information (accounting for the sum of detectable and assignable mass peak intensity) it aligns with the median 20% of microbial contribution to mineral-associated organic matter in arable soils based on a C/N mixing model (Chang et al., 2024) but are lower than amino sugar-based estimates of NM contribution in arable soils (40-80% of SOC, average 50%). However, ratios of FNM over BNM contribution across RT segments ranged from 0 to >4 in UF soil and 0.1 to 3 in FYM soil WEOM, approaching a reported ratio of FNM-C/ BNM-C of ~3 in agricultural soils (Liang et al., 2019) indicating a possible application to use the molecular-level data to constrain (relative) NM contribution to stable SOM.

Our observation of a relatively low overlap of NM markers with soil WEOM could be due to the strong polarity separation of WEOM in our study which provides double resolution on the polarity and mass scale, thereby excluding false overlap between WEOM fingerprints (Adamczyk et al., 2024). 82.9% and 93.6% of cumulative intensity across the polarity range were unexplained by any of our NM markers in FYM and UF soil WEOM, respectively. A possible reason for the large number of compounds left unassigned to any of the sources is a lack of a comprehensive reference database of NM fingerprints that would cover different organisms and NM decomposition stages (Camenzind et al., 2023). Here, we chose only three representative NM types to cover the range of various NM sources, and used fresh, undecomposed NM materials. However, looking at metabolic signals detected in at least two out of the three NMs here (uNM), we only found 0-7% (average, 1.5%) or 1-15% (5.1%) overlap across the polarity range.

Importantly, the NM markers found in soil WEOM only represented a fifth of the overall measured intensity of their original NM spectra (BNM, 19%; FNM, 23%; PNM, 22%), leaving about 80% of signals undetected in soil WEOM, despite being water-soluble. This may indicate that up to 80% of leachable NM compounds are removed during (long-term) SOM formation, by processes such as respiration, leaching, or mineral sorption, and are hence not detectable in soil WEOM (Lützow et al., 2006). This process, constant recycling of bio- and necromass within soils (as well as the oceanic carbon pools) through microbes has been coined the microbial carbon pump (MCP) and used to explain the formation of persistent reduced carbon within mostly oxic environments (Jiao et al., 2010; Liang and Balser, 2011; Lechtenfeld et al., 2015; Kästner and Miltner, 2018). In fact, the NOSC values of molecules found only in NM were, by tendency, higher for BNM and FNM and lower for PNM (Figure S16) as compared to the NM molecules also found in soil WEOM. This could indicate the usage and recycling of NM compounds with lower energy contents, but it could also relate to other removal mechanisms (sorption, etc.).

Finally, WEOM represents only a fraction of all SOM and is more processed, oxidized and lower in molecular weight as compared to bulk SOM. The overlap with undecomposed NM may expectedly be relatively small. Our data, however, show that a large fraction of low molecular weight WEOM is relatively nonpolar and reduced (late RT segments in Fig. 2, Fig. 3c) and that NM contributes mainly to this fraction even in non-fertilized soil WEOM (Fig. 4a, c). Which indicates that even due to the nonpolar nature of NM we can use WEOM as a indicative proxy for NM fingerprinting within SOM.

All in all, LC-FT-ICR-MS enabled the detection of 194 and 377 unique fungal and bacterial markers, respectively (Figure 6), as well as ~5000 plant markers and ~850 shared markers (uNM, Fig. S17). These numbers suggest that the diversity of soluble microbial metabolites is much lower than that of plant material, related to an overall more hydrophobic chemical composition of microbial necromasses. The large range of microbial NM markers in comparison to classical bacterial and fungal biomarkers highlights the added benefit of LC-FT-ICR-MS for constraining microbial imprints in soils. Classical biomarker such as amino sugars or ergosterol are extracted from soils by acid hydrolysis or organic solvents, respectively (Joergensen, 2018; Adamczyk et al., 2024). The intermediate position of the

water-extractable necromass markers between lipidic or carbohydrate-related markers now provides access to an additional set of actively cycled metabolites with a wide range of polarities (uNM markers; Fig S17 b). These additional metabolites were accessible without harsh chemical treatment or organic solvent extraction. To structurally confine these novel necromass markers, FT-ICR-MS fragmentation experiments could be conducted. Tandem MS can help to elucidate structural motifs within SOM (Simon et al., 2022; DiDonato et al., 2023). This could enable not only the detection of shifts in the molecular composition of SOM during substrate decomposition but also the recognition of alterations in structural motifs associated with specific necromass types (Salas et al., 2024).

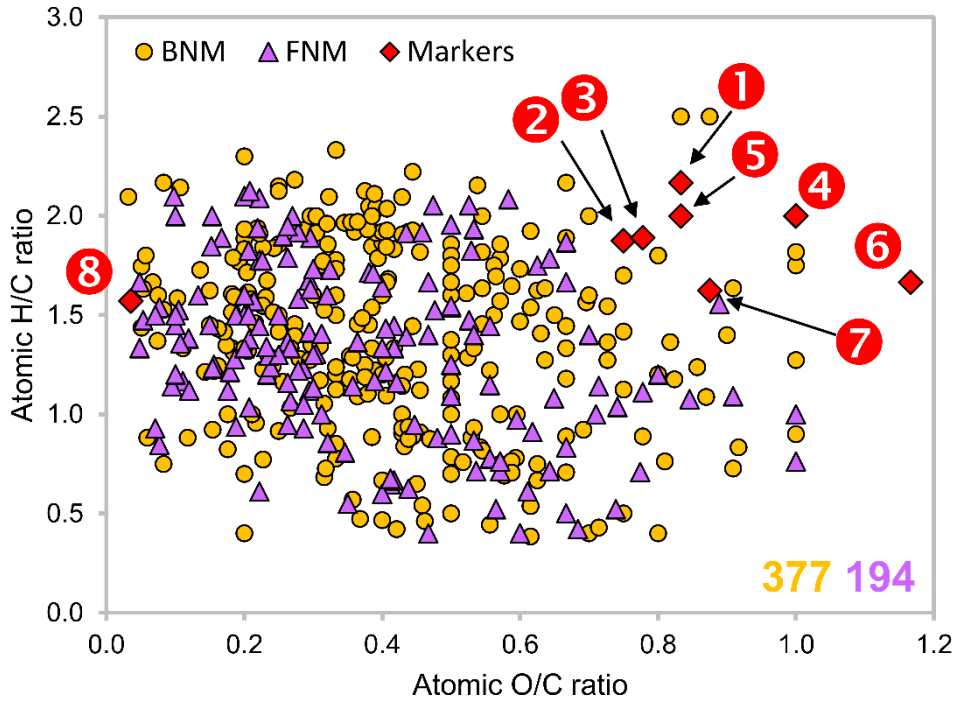

Figure 6: H/C-ratio against O/C-ratio for the sets of unique bacterial (BNM, yellow dots) and fungal (FNM, lilac triangles) necromass markers detected in FYM-receiving soil WEOM depicted in the molecular hydrogen to carbon (H/C) and oxygen to carbon (O/C) compositional space. Numbers refer to the total number of molecular formulas in each set. Commonly employed necromass markers discussed in the literature are shown for reference as red diamonds (Glaser et al., 2004; Joergensen, 2018; Salas et al., 2023, 2024; Adamczyk et al., 2024): Amino sugars: ❶ Galactosamine/ Glucosamine/ Mannosamine; ❷ N-Acetyl-Galactosamine/ N-Acetyl-Glucosamine/ N-Acetyl-Mannosamine; ❸ Muramic acid; Sugars: ❹ Ribose/ Arabinose/ Xylose/ Glucose/ Galactose/ Mannose; ❺ Rhamnose/ Fucose; Uronic acids: ❻ Galacturonic acid/ Glucoronic acid ❼ Talosaminuronic acid; Others: ❽ Ergosterol.

4.4. WEOM oxidation state is driven by compounds unrelated to necromasses

Despite larger overlap with NM markers of virtually all types and across all RT segments, the higher oxidation state of WEOM was mainly driven by the contribution of compounds not related to any of the NM fingerprints (Figure 5). This difference in NOSC between FYM-application and UF can be explained by two, potentially co-occurring processes:

1) Release of stabilized SOM, that is mobilised due to an increase in microbial and enzyme activity and a corresponding higher demand in energy and C that FYM itself cannot meet despite its highly available C and N content (Murphy et al., 2015). This would indicate priming of SOM via FYM addition (Gerzabek et al., 1997). Many studies have shown that the input of bioavailable OM to soil can stimulate SOC mineralization (Kuzyakov et al., 2000; Fontaine et al., 2007; Kuzyakov, 2010). The compounds provided by FYM; can be used to provide the energy needed to maintain the microbe pool within soils.

The increase in microbial bio- and necromass may therefore come at the expense of a stronger turnover of SOM in general, and seems to favour the leaching of compounds low in energetic potential (higher NOSC). Whether this effect may outweigh the benefit of increasing long-term SOC contents, along with other risks of nutrient leaching losses and N_2O emissions, should be investigated in more detail in future (Poulton et al., 2018).

2) Production of molecules from metabolically active microbes that remain undetected in necromass extracts. Of note, many of the compounds in WEOM not assigned to any of the NM fingerprints could also be indicative of other NM types (see above), but the small overlap even with NM markers suggests that also other processes (e.g. accumulation of persistent organic molecules due to microbial turnover) must induce this large shift in NOSC. It has been shown before, that within carbon turnover considerations in line with the theory of the soil microbial carbon pump (MCP) described mechanistic pathways of metabolic turnover of C unrelated and therefore not measurable with a NM fingerprinting approach pal a role (Liang and Balser, 2011; Jiao et al., 2024).

To disentangle both process further experiments that reflect the continuous degradation of NMs are required.

Conclusion

We identified the molecular differences between farmyard manure-receiving and non-receiving soils and characterized distinct markers of three major necromass types (plant, fungal, bacterial) and their contribution to extractable SOM. The difference between FYM receiving soils and controls was explained by an increased presence of necromass-derived compounds, but also show that a large portion of WEOM was not accounted for by necromass-derived compounds. The fact that a majority of molecules unrelated to NM explained shifts to a higher NOSC suggests that the increased activity of microbes and hence, the production of necromass, may come at the expense of stronger oxidation of SOM. This could lead to increased leaching losses of compounds with lower energetic potential, which may be easily oxidized due to their favourable energetic properties. Further research efforts are required to investigate this potential risk of long-term FYM addition to soils.

Acknowledgements

This work is based on data obtained within the DFG Priority Program 2322 “SoilSystems” (project number 441899689). We thank the staff of the core projects, the SPP office and the BExIS team for their work in maintaining the project infrastructure, and the SPP Scientific Committee for their role in setting up the SPP project. KS and CS receive funding from the German Research Foundation (DFG), priority programme 2322. AM and TM were funded by the DFG with the projects (MI 598/9-1; MA 3746/8-1; MA 3746/9-1). Sven Pauler and Tabea Schmidgall is thanked for the help optimizing and producing the bacterial necromass. Soils were provided by S.J. Seidel and H. Hüging (University of Bonn, Germany), C. Resseguier and S. Houot (INRAe, France), K. Schweitzer and M. Baumecker (Humboldt-Universität zu Berlin, Germany), J. Mayer and H.U. Zbinden (Agroscope, Switzerland). We thank Marion Schrumpf, Marco Pöhlmann, Nadine Hempel and Agnes Fastnacht for providing maize straw and Anja Miltner for providing bacterial necromass. We are thankful for using the analytical facilities of ProVIS - Centre for Chemical Microscopy within the Helmholtz Centre for Environmental Research supported by the European Regional Development Funds (EFRE - Europe funds Saxony) and the Helmholtz Association.

Competing Interest Statement

The authors declare no competing interests.

CRediT statement (Contributor Roles Taxonomy)

Konstantin Stumpf (Data curation, Formal analysis, Investigation, Visualization, Writing – original draft), Carsten Simon (Conceptualization, Supervision, Writing – original draft, Writing – review & editing), Anja Miltner (Resources, Writing – review & editing), Thomas Maskow (Resources, Writing – review & editing), Oliver Lechtenfeld (Conceptualization, Supervision, Funding acquisition, Writing – review & editing).

References

Adamczyk, S., Lehtonen, A., Mäkipää, R., Adamczyk, B., 2024. A step forward in fungal biomass estimation – a new protocol for more precise measurements of soil ergosterol with liquid chromatography-mass spectrometry and comparison of extraction methods. New Phytologist 241, 2333–2336. doi:10.1111/nph.19450

Allison, S.D., Hanson, C.A., Treseder, K.K., 2007. Nitrogen fertilization reduces diversity and alters community structure of active fungi in boreal ecosystems. Soil Biology and Biochemistry 39, 1878–1887. doi:10.1016/j.soilbio.2007.02.001

Angst, G., Mueller, K.E., Nierop, K.G.J., Simpson, M.J., 2021. Plant- or microbial-derived? A review on the molecular composition of stabilized soil organic matter. Soil Biology and Biochemistry 156, 108189. doi:10.1016/j.soilbio.2021.108189

Bahureksa, W., Tfaily, M.M., Boiteau, R.M., Young, R.B., Logan, M.N., McKenna, A.M., Borch, T., 2021. Soil Organic Matter Characterization by Fourier Transform Ion Cyclotron Resonance Mass Spectrometry (FTICR MS): A Critical Review of Sample Preparation, Analysis, and Data Interpretation. Environmental Science & Technology 55, 9637–9656. doi:10.1021/acs.est.1c01135

Boer, W. de, Folman, L.B., Summerbell, R.C., Boddy, L., 2005. Living in a fungal world: impact of fungi on soil bacterial niche development. FEMS Microbiology Reviews 29, 795–811. doi:10.1016/j.femsre.2004.11.005

Bolinder, M.A., Crotty, F., Elsen, A., Frac, M., Kismányoky, T., Lipiec, J., Tits, M., Tóth, Z., Kätterer, T., 2020. The effect of crop residues, cover crops, manures and nitrogen fertilization on soil organic carbon changes in agroecosystems: a synthesis of reviews. Mitigation and Adaptation Strategies for Global Change 25, 929–952. doi:10.1007/s11027-020-09916-3

Brailsford, F.L., Glanville, H.C., Golyshin, P.N., Marshall, M.R., Lloyd, C.E., Johnes, P.J., Jones, D.L., 2019. Nutrient enrichment induces a shift in dissolved organic carbon (DOC) metabolism in oligotrophic freshwater sediments. The Science of the Total Environment 690, 1131–1139. doi:10.1016/j.scitotenv.2019.07.054

Brown, R.W., Chadwick, D.R., Zang, H., Jones, D.L., 2021. Use of metabolomics to quantify changes in soil microbial function in response to fertiliser nitrogen supply and extreme drought. Soil Biology and Biochemistry 160. doi:10.1016/j.soilbio.2021.108351

Brown, R.W., Reay, M.K., Centler, F., Chadwick, D.R., Bull, I.D., McDonald, J.E., Evershed, R.P., Jones, D.L., 2024. Soil metabolomics - current challenges and future perspectives. Soil Biology and Biochemistry 193, 109382. doi:10.1016/j.soilbio.2024.109382

Buckeridge, K.M., Creamer, C., Whitaker, J., 2022. Deconstructing the microbial necromass continuum to inform soil carbon sequestration. Functional Ecology 36, 1396–1410. doi:10.1111/1365-2435.14014

Camenzind, T., Mason-Jones, K., Mansour, I., Rillig, M.C., Lehmann, J., 2023. Formation of necromass-derived soil organic carbon determined by microbial death pathways. Nature Geoscience 1–8. doi:10.1038/s41561-022-01100-3

Chang, E.-H., Chung, R.-S., Tsai, Y.-H., 2007. Effect of different application rates of organic fertilizer on soil enzyme activity and microbial population. Soil Science & Plant Nutrition 53, 132–140. doi:10.1111/j.1747-0765.2007.00122.x

Chang, Y., Sokol, N.W., Van Groenigen, K.J., Bradford, M.A., Ji, D., Crowther, T.W., Liang, C., Luo, Y., Kuzyakov, Y., Wang, J., Ding, F., 2024. A stoichiometric approach to estimate sources of mineral-associated soil organic matter. Global Change Biology 30, e17092. doi:10.1111/gcb.17092

Craig, M.E., Turner, B.L., Liang, C., Clay, K., Johnson, D.J., Phillips, R.P., 2018. Tree mycorrhizal type predicts within-site variability in the storage and distribution of soil organic matter. Global Change Biology 24, 3317–3330. doi:10.1111/gcb.14132

Del Giorgio, P.A., Cole, J.J., 1998. BACTERIAL GROWTH EFFICIENCY IN NATURAL AQUATIC SYSTEMS. Annual Review of Ecology and Systematics 29, 503–541. doi:10.1146/annurev.ecolsys.29.1.503

DiDonato, N., Rivas-Ubach, A., Kew, W., Clendinen, C., Sokol, N., Kyle, J.E., Martínez, C.E., Foley, M.M., Tolić, N., Pett-Ridge, J., Paša-Tolić, L., 2023. Improved characterization of soil organic matter by integrating FTICR-MS, liquid chromatography tandem mass spectrometry and molecular networking: a case study of root litter decay under drought conditions. doi:10.1101/2023.06.20.545455

Ellerbrock, R.H., Höhn, A., Gerke, H.H., n.d. Characterization of soil organic matter from a sandy soil in relation to management practice using FT-IR spectroscopy.

Fan, Z., Liang, C., 2015. Significance of microbial asynchronous anabolism to soil carbon dynamics driven by litter inputs. Scientific Reports 5, 9575. doi:10.1038/srep09575

Fontaine, S., Barot, S., Barré, P., Bdioui, N., Mary, B., Rumpel, C., 2007. Stability of organic carbon in deep soil layers controlled by fresh carbon supply. Nature 450, 277–280. doi:10.1038/nature06275

Gerzabek, M. h., Pichlmayer, F., Kirchmann, H., Haberhauer, G., 1997. The response of soil organic matter to manure amendments in a long-term experiment at Ultuna, Sweden. European Journal of Soil Science 48, 273–282. doi:10.1111/j.1365-2389.1997.tb00547.x

Glaser, B., Turrión, M.-B., Alef, K., 2004. Amino sugars and muramic acid—biomarkers for soil microbial community structure analysis. Soil Biology and Biochemistry 36, 399–407. doi:10.1016/j.soilbio.2003.10.013

Guggenberger, G., Frey, S.D., Six, J., Paustian, K., Elliott, E.T., 1999. Bacterial and Fungal Cell-Wall Residues in Conventional and No-Tillage Agroecosystems. Soil Science Society of America Journal 63, 1188–1198. doi:10.2136/sssaj1999.6351188x

Guigue, J., Harir, M., Mathieu, O., Lucio, M., Ranjard, L., Lévêque, J., Schmitt-Kopplin, P., 2016. Ultrahigh-resolution FT-ICR mass spectrometry for molecular characterisation of pressurised hot water-extractable organic matter in soils. Biogeochemistry 128, 307–326. doi:10.1007/s10533-016-0209-5

Gunina, A., Kuzyakov, Y., 2022. From energy to (soil organic) matter. Global Change Biology 28, 2169–2182. doi:10.1111/gcb.16071

Hall, S.J., Ye, C., Weintraub, S.R., Hockaday, W.C., 2020. Molecular trade-offs in soil organic carbon composition at continental scale. Nature Geoscience 13, 687–692. doi:10.1038/s41561-020-0634-x

Han, L., Kaesler, J., Peng, C., Reemtsma, T., Lechtenfeld, O.J., 2021. Online counter gradient LC-FT-ICR-MS enables detection of highly polar natural organic matter fractions. Analytical Chemistry 93, 1740–1748. doi:10.1021/acs.analchem.0c04426

Hertkorn, N., Frommberger, M., Witt, M., Koch, B.P., Schmitt-Kopplin, Ph., Perdue, E.M., 2008. Natural Organic Matter and the Event Horizon of Mass Spectrometry. Analytical Chemistry 80, 8908–8919. doi:10.1021/ac800464g

Herzsprung, P., Hertkorn, N., von Tümpling, W., Harir, M., Friese, K., Schmitt-Kopplin, P., 2014. Understanding molecular formula assignment of Fourier transform ion cyclotron resonance mass spectrometry data of natural organic matter from a chemical point of view. Analytical and Bioanalytical Chemistry 406, 7977–7987. doi:10.1007/s00216-014-8249-y

Hu, W., Zhang, Y., Rong, X., Zhou, X., Fei, J., Peng, J., Luo, G., 2024. Biochar and organic fertilizer applications enhance soil functional microbial abundance and agroecosystem multifunctionality. Biochar 6, 3. doi:10.1007/s42773-023-00296-w

Jennings, E., Kremser, A., Han, L., Reemtsma, T., Lechtenfeld, O.J., 2022. Discovery of Polar Ozonation Byproducts via Direct Injection of Effluent Organic Matter with Online LC-FT-ICR-MS. Environmental Science & Technology 56, 1894–1904. doi:10.1021/acs.est.1c04310

Jiao, N., Herndl, G.J., Hansell, D.A., Benner, R., Kattner, G., Wilhelm, S.W., Kirchman, D.L., Weinbauer, M.G., Luo, T., Chen, F., Azam, F., 2010. Microbial production of recalcitrant dissolved organic matter: Long-term carbon storage in the global ocean. Nature Reviews Microbiology 8, 593–599. doi:10.1038/nrmicro2386

Jiao, N., Luo, T., Chen, Q., Zhao, Z., Xiao, X., Liu, J., Jian, Z., Xie, S., Thomas, H., Herndl, G.J., Benner, R., Gonsior, M., Chen, F., Cai, W.-J., Robinson, C., 2024. The microbial carbon pump and climate change. Nature Reviews Microbiology 1–12. doi:10.1038/s41579-024-01018-0

Joergensen, R.G., 2018. Amino sugars as specific indices for fungal and bacterial residues in soil. Biology and Fertility of Soils 54, 559–568. doi:10.1007/s00374-018-1288-3

Kaiser, M., Ellerbrock, R.H., 2005. Functional characterization of soil organic matter fractions different in solubility originating from a long-term field experiment. Geoderma 127, 196–206. doi:10.1016/j.geoderma.2004.12.002

Kalbitz, K., Solinger, S., Park, J.-H., Michalzik, B., Matzner, E., 2000. CONTROLS ON THE DYNAMICS OF DISSOLVED ORGANIC MATTER IN SOILS: A REVIEW. Soil Science 165, 277.

Kästner, M., Miltner, A., 2018. Chapter 5 - SOM and Microbes—What Is Left From Microbial Life, in: Garcia, C., Nannipieri, P., Hernandez, T. (Eds.), The Future of Soil Carbon. Academic Press, pp. 125–163. doi:10.1016/B978-0-12-811687-6.00005-5

Kind, T., Fiehn, O., 2007. Seven Golden Rules for heuristic filtering of molecular formulas obtained by accurate mass spectrometry. BMC Bioinformatics 8, 105. doi:10.1186/1471-2105-8-105

Koch, B.P., Kattner, G., Witt, M., Passow, U., 2014. Molecular insights into the microbial formation of marine dissolved organic matter: recalcitrant or labile? Biogeosciences 11, 4173–4190. doi:10.5194/bg-11-4173-2014

Kögel-Knabner, I., 2002. The macromolecular organic composition of plant and microbial residues as inputs to soil organic matter. Soil Biology and Biochemistry 34, 139–162. doi:10.1016/S0038-0717(01)00158-4

Kögel-Knabner, I., Rumpel, C., 2018. Advances in Molecular Approaches for Understanding Soil Organic Matter Composition, Origin, and Turnover: A Historical Overview, in: Advances in Agronomy. Academic Press Inc., pp. 1–48. doi:10.1016/bs.agron.2018.01.003

Kuzyakov, Y., 2010. Priming effects: Interactions between living and dead organic matter. Soil Biology and Biochemistry 42, 1363–1371. doi:10.1016/j.soilbio.2010.04.003

Kuzyakov, Y., Friedel, J.K., Stahr, K., 2000. Review of mechanisms and quantification of priming effects. Soil Biology and Biochemistry 32, 1485–1498. doi:10.1016/S0038-0717(00)00084-5

LaRowe, D.E., Van Cappellen, P., 2011. Degradation of natural organic matter: A thermodynamic analysis. Geochimica et Cosmochimica Acta 75, 2030–2042. doi:10.1016/j.gca.2011.01.020

Lechtenfeld, O.J., Hertkorn, N., Shen, Y., Witt, M., Benner, R., 2015. Marine sequestration of carbon in bacterial metabolites. Nature Communications 6. doi:10.1038/ncomms7711

Lechtenfeld, O.J., Kaesler, J., Jennings, E.K., Koch, B.P., 2024. Direct Analysis of Marine Dissolved Organic Matter Using LC-FT-ICR MS. Environmental Science & Technology 58, 4637–4647. doi:10.1021/acs.est.3c07219

Lehmann, J., Kleber, M., 2015. The contentious nature of soil organic matter. Nature 528, 60–68. doi:10.1038/nature16069

Liang, C., Amelung, W., Lehmann, J., Kästner, M., 2019. Quantitative assessment of microbial necromass contribution to soil organic matter. Global Change Biology 25, 3578–3590. doi:10.1111/gcb.14781

Liang, C., Balser, T.C., 2011. Microbial production of recalcitrant organic matter in global soils: implications for productivity and climate policy. Nature Reviews Microbiology 9, 75–75. doi:10.1038/nrmicro2386-c1

Liu, K., Ding, X., Wang, J., 2020. Soil metabolome correlates with bacterial diversity and co-occurrence patterns in root-associated soils on the Tibetan Plateau. The Science of the Total Environment 735, 139572. doi:10.1016/j.scitotenv.2020.139572

Lohse, M., Blaser, S.R.G.A., Vetterlein, D., Schlüter, S., Oburger, E., Reemtsma, T., Lechtenfeld, O.J., 2020. Online Nano Solid Phase Extraction Fourier-Transform Ion Cyclotron Resonance Mass Spectrometry Workflow to Analyze Small Scale Gradients of Soil Solution Organic Matter in the Rhizosphere. Analytical Chemistry 92, 10442–10449. doi:10.1021/acs.analchem.0c00946

Lohse, M., Haag, R., Lippold, E., Vetterlein, D., Reemtsma, T., Lechtenfeld, O.J., 2021. Direct Imaging of Plant Metabolites in the Rhizosphere Using Laser Desorption Ionization Ultra-High Resolution Mass Spectrometry. Frontiers in Plant Science 12. doi:10.3389/fpls.2021.753812

Lützow, M. v., Kögel-Knabner, I., Ekschmitt, K., Matzner, E., Guggenberger, G., Marschner, B., Flessa, H., 2006. Stabilization of organic matter in temperate soils: mechanisms and their relevance under different soil conditions – a review. European Journal of Soil Science 57, 426–445. doi:10.1111/j.1365-2389.2006.00809.x

Ma, Q., Wen, Y., Wang, D., Sun, X., Hill, P.W., Macdonald, A., Chadwick, D.R., Wu, L., Jones, D.L., 2020. Farmyard manure applications stimulate soil carbon and nitrogen cycling by boosting microbial biomass rather than changing its community composition. Soil Biology and Biochemistry 144, 107760. doi:10.1016/j.soilbio.2020.107760

Ma, Q., Wu, L., Wang, J., Ma, J., Zheng, N., Hill, P.W., Chadwick, D.R., Jones, D.L., 2018. Fertilizer regime changes the competitive uptake of organic nitrogen by wheat and soil microorganisms: An in-situ uptake test using 13C, 15N labelling, and 13C-PLFA analysis. Soil Biology and Biochemistry 125, 319–327. doi:10.1016/j.soilbio.2018.08.009

Ma, T., Zhu, S., Wang, Z., Chen, D., Dai, G., Feng, B., Su, X., Hu, H., Li, K., Han, W., Liang, C., Bai, Y., Feng, X., 2018. Divergent accumulation of microbial necromass and plant lignin components in grassland soils. Nature Communications 9, 3480. doi:10.1038/s41467-018-05891-1

Maillard, É., Angers, D.A., 2014. Animal manure application and soil organic carbon stocks: a meta-analysis. Global Change Biology 20, 666–679. doi:10.1111/gcb.12438

Malik, A.A., Roth, V.-N., Hébert, M., Tremblay, L., Dittmar, T., Gleixner, G., 2016. Linking molecular size, composition and carbon turnover of extractable soil microbial compounds. Soil Biology and Biochemistry 100, 66–73. doi:10.1016/j.soilbio.2016.05.019

Mao, J., Olk, D.C., Fang, X., He, Z., Schmidt-Rohr, K., 2008. Influence of animal manure application on the chemical structures of soil organic matter as investigated by advanced solid-state NMR and FT-IR spectroscopy. Geoderma 146, 353–362. doi:10.1016/j.geoderma.2008.06.003

Miltner, A., Bombach, P., Schmidt-Brücken, B., Kästner, M., 2012. SOM genesis: microbial biomass as a significant source. Biogeochemistry 111, 41–55. doi:10.1007/s10533-011-9658-z

Moore, J., Mccann, K., Setälä, H., Ruiter, P., 2002. Top-down is bottom-up: Does predation in the rhizosphere regulate above ground production. Ecology 84.

Murphy, C.J., Baggs, E.M., Morley, N., Wall, D.P., Paterson, E., 2015. Rhizosphere priming can promote mobilisation of N-rich compounds from soil organic matter. Soil Biology and Biochemistry 81, 236–243. doi:10.1016/j.soilbio.2014.11.027

Ohno, T., Parr, T.B., Gruselle, M.C.I., Fernandez, I.J., Sleighter, R.L., Hatcher, P.G., 2014. Molecular composition and biodegradability of soil organic matter: A case study comparing two New England forest types. Environmental Science and Technology 48, 7229–7236. doi:10.1021/es405570c

Op De Beeck, M., Troein, C., Peterson, C., Persson, P., Tunlid, A., 2018. Fenton reaction facilitates organic nitrogen acquisition by an ectomycorrhizal fungus. The New Phytologist 218, 335–343. doi:10.1111/nph.14971

Poulton, P., Johnston, J., Macdonald, A., White, R., Powlson, D., 2018. Major limitations to achieving "4 per 1000" increases in soil organic carbon stock in temperate regions: Evidence from long-term experiments at Rothamsted Research, United Kingdom. Global Change Biology 24, 2563–2584. doi:10.1111/gcb.14066

Raeke, J., Lechtenfeld, O.J., Wagner, M., Herzsprung, P., Reemtsma, T., 2016. Selectivity of solid phase extraction of freshwater dissolved organic matter and its effect on ultrahigh resolution mass spectra. Environmental Science: Processes & Impacts 18, 918–927. doi:10.1039/C6EM00200E

Reemtsma, T., These, A., Springer, A., Linscheid, M., 2006. Fulvic Acids as Transition State of Organic Matter: Indications from High Resolution Mass Spectrometry. Environmental Science & Technology 40, 5839–5845. doi:10.1021/es060318c

Roth, V.N., Lange, M., Simon, C., Hertkorn, N., Bucher, S., Goodall, T., Griffiths, R.I., Mellado-Vázquez, P.G., Mommer, L., Oram, N.J., Weigelt, A., Dittmar, T., Gleixner, G., 2019. Persistence of dissolved organic matter explained by molecular changes during its passage through soil. Nature Geoscience 12, 755–761. doi:10.1038/s41561-019-0417-4

Rousk, J., Bååth, E., 2007. Fungal and bacterial growth in soil with plant materials of different C/N ratios: Fungal and bacterial growth with plant materials in soil. FEMS Microbiology Ecology 62, 258–267. doi:10.1111/j.1574-6941.2007.00398.x

Salas, E., Gorfer, M., Bandian, D., Eichorst, S.A., Schmidt, H., Horak, J., Rittmann, S.K.-M.R., Schleper, C., Reischl, B., Pribasnig, T., Jansa, J., Kaiser, C., Wanek, W., 2024. Reevaluation and novel insights into amino sugar and neutral sugar necromass biomarkers in archaea, bacteria, fungi, and plants. Science of The Total Environment 906, 167463. doi:10.1016/j.scitotenv.2023.167463

Salas, E., Gorfer, M., Bandian, D., Wang, B., Kaiser, C., Wanek, W., 2023. A rapid and sensitive assay to quantify amino sugars, neutral sugars and uronic acid necromass biomarkers using pre-column derivatization, ultra-high-performance liquid chromatography and high-resolution mass spectrometry. Soil Biology and Biochemistry 177, 108927. doi:10.1016/j.soilbio.2022.108927

Schmidt, M.W.I., Torn, M.S., Abiven, S., Dittmar, T., Guggenberger, G., Janssens, I.A., Kleber, M., Kögel-Knabner, I., Lehmann, J., Manning, D.A.C., Nannipieri, P., Rasse, D.P., Weiner, S., Trumbore, S.E., 2011. Persistence of soil organic matter as an ecosystem property. Nature 478, 49–56. doi:10.1038/nature10386

Schweigert, M., Herrmann, S., Miltner, A., Fester, T., Kästner, M., 2015. Fate of ectomycorrhizal fungal biomass in a soil bioreactor system and its contribution to soil organic matter formation. Soil Biology and Biochemistry 88, 120–127. doi:10.1016/j.soilbio.2015.05.012

Sharma, P., Laor, Y., Raviv, M., Medina, S., Saadi, I., Krasnovsky, A., Vager, M., Levy, G.J., Bar-Tal, A., Borisover, M., 2017. Green manure as part of organic management cycle: Effects on changes in organic matter characteristics across the soil profile. Geoderma 305, 197–207. doi:10.1016/j.geoderma.2017.06.003

Simon, C., Dührkop, K., Petras, D., Roth, V.-N., Böcker, S., Dorrestein, P., Gleixner, G., 2022. Mass difference matching unfolds hidden molecular structures of dissolved organic matter (preprint). Chemistry. doi:10.26434/chemrxiv-2021-cxxt1-v3

Simon, C., Miltner, A., Mulder, I., Kaiser, K., Lorenz, M., Thiele-Bruhn, S., Lechtenfeld, O.J., 2024. Long-term effects of farmyard manure addition on soil organic matter molecular composition: C transformation as a major driver of energetic potential. doi:10.21203/rs.3.rs-4542343/v1

Simpson, A.J., Simpson, M.J., Smith, E., Kelleher, B.P., 2007. Microbially Derived Inputs to Soil Organic Matter: Are Current Estimates Too Low? Environmental Science & Technology 41, 8070–8076. doi:10.1021/es071217x

Swenson, T.L., Jenkins, S., Bowen, B.P., Northen, T.R., 2015. Untargeted soil metabolomics methods for analysis of extractable organic matter. Soil Biology and Biochemistry 80, 189–198. doi:10.1016/j.soilbio.2014.10.007

Tang, S., Ma, Q., Zhou, J., Pan, W., Chadwick, D.R., Gregory, A.S., Wu, L., Jones, D.L., 2023. Use of untargeted metabolomics to analyse changes in extractable soil organic matter in response to long-term fertilisation. Biology and Fertility of Soils 59, 301–316. doi:10.1007/s00374-023-01706-8

Tarnocai, C., Canadell, J., Schuur, E., Kuhry, P., Mazhitova, G., Zimov, S., 2009. Soil Organic Carbon Pools in the Northern Circumpolar Permafrost Region. Global Biogeochem. Cycles 23. doi:10.1029/2008GB003327

Tfaily, M.M., Chu, R.K., Tolić, N., Roscioli, K.M., Anderton, C.R., Paša-Tolić, L., Robinson, E.W., Hess, N.J., 2015. Advanced solvent based methods for molecular characterization of soil organic matter by high-resolution mass spectrometry. Analytical Chemistry 87, 5206–5215. doi:10.1021/acs.analchem.5b00116

Thangarajan, R., Bolan, N.S., Tian, G., Naidu, R., Kunhikrishnan, A., 2013. Role of organic amendment application on greenhouse gas emission from soil. Science of the Total Environment 465, 72–96. doi:10.1016/j.scitotenv.2013.01.031

Wang, B., An, S., Liang, C., Liu, Y., Kuzyakov, Y., 2021. Microbial necromass as the source of soil organic carbon in global ecosystems. Soil Biology and Biochemistry 162, 108422. doi:10.1016/j.soilbio.2021.108422

Withers, E., Hill, P.W., Chadwick, D.R., Jones, D.L., 2020. Use of untargeted metabolomics for assessing soil quality and microbial function. Soil Biology and Biochemistry 143, 107758. doi:10.1016/j.soilbio.2020.107758

Wu, H., Wan, S., Ruan, C., Wan, W., Han, M., Chen, G., Liu, Y., Zhu, K., Liang, C., Wang, G., 2023. Soil microbial necromass: The state-of-the-art, knowledge gaps, and future perspectives. European Journal of Soil Biology 115, 103472. doi:10.1016/j.ejsobi.2023.103472

Wurz, J., Groß, A., Franze, K., Lechtenfeld, O., 2024. Lambda-Miner: Enhancing Reproducible Natural Organic Matter Data Processing with a Semi-Automatic Web Application (No. EGU24-15782). Presented at the EGU24, Copernicus Meetings. doi:10.5194/egusphere-egu24-15782

Zhang, X., Chen, Z., Huo, X., Kang, J., Zhao, S., Peng, Y., Deng, F., Shen, J., Chu, W., 2021. Application of Fourier transform ion cyclotron resonance mass spectrometry in deciphering molecular composition of soil organic matter: A review. Science of the Total Environment 756. doi:10.1016/j.scitotenv.2020.144140